Naval Research Laboratory
Washington, DC 20375-5320

NRL/7320/FR--2021/1

Nonlinear Data Assimilation for Ocean Forecasting

JOHN OSBORNE

Ocean Dynamics and Prediction
Ocean Sciences Division

March 8, 2021

REPORT DOCUMENTATION PAGE

Form Approved
OMB No. 0704-0188

1. REPORT DATE *(DD-MM-YYYY)*	2. REPORT TYPE	3. DATES COVERED *(From - To)*
10-08-2020	NRL Formal Report	08-07-2019 to 07-07-2020

4. TITLE AND SUBTITLE
Nonlinear Data Assimilation for Ocean Forecasting

5a. CONTRACT NUMBER

5b. GRANT NUMBER

5c. PROGRAM ELEMENT NUMBER
NISE

6. AUTHOR(S)
John Osborne

5d. PROJECT NUMBER
73-6C03-C-0-5

5e. TASK NUMBER

5f. WORK UNIT NUMBER
6C03

7. PERFORMING ORGANIZATION NAME(S) AND ADDRESS(ES)
Naval Research Laboratory
4555 Overlook Avenue, SW
Washington, DC 20375-5320

8. PERFORMING ORGANIZATION REPORT NUMBER
NRL/7320/FR--2021/1

9. SPONSORING / MONITORING AGENCY NAME(S) AND ADDRESS(ES)
Naval Research Laboratory
4555 Overlook Avenue, SW
Washington, DC 20375-5320

10. SPONSOR/MONITOR'S ACRONYM(S)
NRL-NISE

11. SPONSOR/MONITOR'S REPORT NUMBER(S)

12. DISTRIBUTION / AVAILABILITY STATEMENT
Distribution Statement A: Approved for public release. Distribution is unlimited.

13. SUPPLEMENTARY NOTES
Karles Fellowship

14. ABSTRACT

This report presents research conducted in investigating a non-linear data assimilation method, "diffusive back and forth nudging" (DBFN). DBFN may be able to reduce errors like four-dimensional variational assimilation, the most advanced data assimilation method, but at greatly reduced computational cost.
DBFN works by running a model forwards and backwards in time with an additional "nudging" term that updates the ocean model with information from observations per a prescribed covariance. DBFN is tested here in two simple dynamical systems. Results are promising and demonstrate a need for further research.

15. SUBJECT TERMS
Ocean forecasting, Data assimilation, Non-linear data assimilation, nudging, back and forth nudging, four-dimensional variational assimilation, 4DVAR, three-dimensional variational assimilation, 3DVAR

16. SECURITY CLASSIFICATION OF:			17. LIMITATION OF ABSTRACT	18. NUMBER OF PAGES	19a. NAME OF RESPONSIBLE PERSON
a. REPORT	b. ABSTRACT	c. THIS PAGE	SAR	16	John Osborne
Unclassified	Unclassified	Unclassified			19b. TELEPHONE NUMBER *(include area code)* (228) 688-4708

Standard Form 298 (Rev. 8-98)
Prescribed by ANSI Std. Z39.18

This page intentionally left blank

CONTENTS

This page intentionally left blank

EXECUTIVE SUMMARY

Ocean forecasting is difficult due to the ocean's inherent chaotic nature and the errors present in forecast initial conditions, boundary conditions, forcing, and model physics. Data assimilation is a process that combines observations and recent forecasts to create new, accurate forecasts. Data assimilation is computationally expensive, often more expensive than producing the forecast alone. Data assimilation methods that reduce error or computational cost are of interest.

This report presents research conducted in investigation of a nonlinear data assimilation method, "diffusive back and forth nudging" (DBFN). DBFN may be able to reduce errors like the most advanced data assimilation methods but at reduced computational cost. DBFN works by running a model forwards and backwards in time with an additional "nudging" term. It can be relatively simple to implement. The nudging term updates the ocean model with information from observations per a prescribed covariance. DBFN is tested here in two simple dynamical systems. Results are promising and demonstrate a need for further research.

This page intentionally left blank

NONLINEAR DATA ASSIMILATION FOR OCEAN FORECASTING

1. INTRODUCTION

Accurately forecasting the ocean via numerical models is difficult due to the ocean's chaotic nature and models' use of erroneous initial conditions, boundary conditions, surface forcing, and physics. Data assimilation is the process that combines observations with model results given selected constraints (e.g., Bennett 2002, Evensen 1994) and is widely used for ocean forecasting (e.g., Sakov et al. 2012, Cummings and Smedstad 2013, Oke et al. 2013). In real-time ocean forecasting, data assimilation is used to correct the most recent forecast with observations available after that forecast was issued. This produces an "analysis" which is used to initialize the next forecast. There are multiple data assimilation methods and practical considerations impact the choice of data assimilation method. Forecasts must be produced in a timely manner on limited computer resources but also must be accurate enough to be useful. For regions of great interest, very low errors are desired, usually achieved by running at higher resolution but at higher computational cost. New methods that improve accuracy or reduce computational cost are of interest.

Methods currently used for the Navy's ocean models include three-dimensional (3DVAR; Cummings and Smedstad 2013, Daley and Barker 2001) and four-dimensional variational assimilation (4DVAR; Ngodock and Carrier 2014). Ensemble approaches are under study (Coehlo et al. 2009, Wei et al. 2016, Ngodock et al. 2020). 3DVAR has relatively lower computational cost than 4DVAR, but 3DVAR forecast errors can be higher by 10% or more.

A data assimilation method that could improve upon current methods is a nonlinear approach, referred to as "diffusive back and forth nudging" (DBFN; Auroux et al. 2011). It may offer forecast errors like 4DVAR with reduced computational cost (Ruggerio et al. 2016). Like 4DVAR, it runs forwards and backwards in time, but it uses the full model, not the adjoint and tangent linear models of 4DVAR. This offers two advantages. One advantage comes at run time. The full model is less expensive to run than one iteration of the adjoint and tangent linear models, needing 10% to 20% of the run time (Ruggerio et al. 2016). Given computational concerns, this is valuable in multiple ways (enabling higher resolution for the same computational cost, reallocating resources to other efforts, or simply providing a forecast in a timelier manner). The second advantage comes in development and maintenance. Adjoint and tangent linear models are time-consuming to develop and maintain, as they work with a larger, modified version of the original model physics. Because DBFN uses the original model physics, careful construction of the model, with an explicit time-stepping algorithm, enab[1]les implementing DBFN with less effort in development and maintenance.

The Navy uses two ocean models with data assimilation: the Navy Coastal Ocean Model (NCOM; Martin 2000, Barron et al. 2006) for regional ocean modeling, and the Hybrid Coordinate Model (HYCOM; Bleck 2002, Metzger et al. 2017). Both 3DVAR (Smith et al. 2017, Rowley and Mask 2014) and 4DVAR data assimilation (Ngodock and Carrier 2014) are available for NCOM. In contrast, for HYCOM, only 3DVAR (Metzger et al. 2017) is available. Both models are large and complex and implementing DBFN in either is beyond the scope of this project. Because of this, DBFN's benefits and costs are examined here with relatively simple models.

Section 2 details the method. Section 3 describes the implementation and testing of the method for the advection equation. Section 4 describes the implementation and testing of the method for the Lorenz 05 model, a chaotic dynamical system. Section 5 summarizes results.

Manuscript approved February 25, 2021.

2. METHOD: DIFFUSIVE BACK AND FORTH NUDGING

DBFN was introduced as an extension of back and forth nudging (e.g., Auroux and Blum 2005), first appearing in Luenberger (1966). The DBFN algorithm is relatively simple. Assume we have a time-continuous system with dynamics given by

$$\partial_t X = F(X) + \upsilon \Delta X, 0 < t < T, \tag{1}$$

where X is the model state (with initial condition $X_0 = X(t = 0)$), F is the model operator (including spatial derivatives but not diffusion operators), υ is the diffusion coefficient, ∂_t denotes the partial derivative with respect to time, and Δ is the diffusion operator (assumed here to be a Laplacian). Analytical equations describing ocean circulation may not explicitly include diffusion. However, the numerical schemes for ocean circulation often do have diffusion for stability and subscale processes, and so it is considered here.

With this model, the DBFN framework is

$$\begin{cases} \partial_t X_k = F(X_k) + \upsilon \Delta X_k + G\big(Y - H(X_k)\big) \\ X_k(0) = \overleftarrow{X}_{k-1}(0), 0 < t < T \end{cases} \tag{2}$$

$$\begin{cases} \partial_t \overleftarrow{X}_k = F\big(\overleftarrow{X}_k\big) - \upsilon \Delta X_k - G'(Y - H\overleftarrow{X}_k) \\ \overleftarrow{X}_k(T) = X_k(T), T > t > 0 \end{cases}, \tag{3}$$

where H is the observation operator, Y denotes observations, G and G' are the gain matrices, and $\overleftarrow{X}$ is the model state from the backward-nudge formulation. The iteration of the system is denoted by k, $k > 0$. Eq. (2) is the forward nudge and Eq. (3) is the backward nudge. For the second and later analysis-forecast cycles, initialize the forward nudge with the final time step from the prior forecast.

At this point, in Eq. (3), subtraction of the diffusive term makes Eq. (3) ill-posed. Recasting the time variable overcomes this. Define $t' = T - t$. Then, Eq. (3) becomes

$$\begin{cases} \partial_t \overleftarrow{X}_k = -F\big(\overleftarrow{X}_k\big) + \upsilon \Delta X_k + G'(Y - H\overleftarrow{X}_k) \\ \overleftarrow{X}_k(t' = 0) = X_k(T), 0 < t' < T \end{cases}, \tag{4}$$

and Eq. (4) is well-posed. Note that while F is acting backwards with respect to t, the diffusion term is not. So, diffusion continues when the system runs backwards. This will impact results, as seen in sections 3 and 4.

Convergence of the system can be set several ways (Ruggerio et al. 2016), e.g., root-mean-square difference of successive forward nudges below a threshold. Alternatively, the number of iterations can be limited.

3. DBFN FOR THE ADVECTION EQUATION

As a first step, DBFN is implemented for the advection equation using a diffusive numerical scheme. The advection equation is simple, but this offers benefits. Exact solutions for the advection equation are available via the method of characteristics, which enables computing exact errors. Testing a simple equation also allows for simplified testing of Eq. (4), the recast version of the backwards nudge.

The advection equation describes transport of a conserved quantity by a velocity field. In one dimension, the advection equation is

$$\partial_t q(x,t) = -u\partial_x q(x,t), \tag{5}$$

where q is the conserved quantity (e.g., a non-reactive dye in fluid) and u is the velocity. Here, we pick $u = 0.5$, the spatial domain as $0 < x < 1$ with periodic boundary conditions, and the time domain as $0 < t < 6$. The period of this system is 6 units (e.g., seconds). The advection equation does not have a diffusive term and is seemingly a poor fit for studying DBFN. However, if the system is modeled with the upwind scheme, a diffusive term can be found via the method of modified equations (e.g., LeVeque 2002).

Following LeVeque (2002), the upwind method is first-order accurate for the advection equation. The explicit time-stepping formulation is

$$q_k^{n+1} = q_k^n - \frac{u\Delta t}{\Delta x}(q_k^n - q_{k-1}^n) + \mathcal{O}(\Delta x, \Delta t), \tag{6}$$

where Δt and Δx are the selected time and grid steps and $q_k^n = q(k\Delta x, n\Delta t)$. Let $\hat{q}$ be an exact solution of Eq. (6). Then it can be shown that

$$\hat{q} = -u\hat{q}_x + \frac{1}{2}(u\Delta x - u^2\Delta t)\hat{q}_{xx} + \mathcal{O}(\Delta x^2, \Delta t^2), \tag{7}$$

which has a diffusive term. Thus, as described previously, we have a non-diffusive system in Eq. (5) which has a diffusive numerical approximation in Eq. (7). In this case, the viscosity is prescribed by u and the time- and space-step sizes, i.e., $\nu = \frac{1}{2}(u\Delta x - u^2\Delta t)$. Three of ν, u, Δx, and Δt may be picked, but the choices also must satisfy the Courant-Fredricks-Levy condition, $u\Delta t/\Delta x < 1$ (Courant, Fredricks, and Levy 1928).

Before numerically implementing the system, we briefly review what the DBFN equations are for Eq. (7). The forward nudge is

$$\partial_t q_k = -\frac{1}{2}\partial_x q_k + \nu\partial_{xx} q_k + G(q^N - q_k) \tag{8}$$

and the backward nudge is

$$\partial_t \tilde{q}_k = +\frac{1}{2}\partial_x \tilde{q}_k + \nu\partial_{xx} \tilde{q}_k + G'(q^N - \tilde{q}_k). \tag{9}$$

Note that the forward nudge and the backward nudge are identical, except for the sign of the advective term. To simplify implementation, computation of the advective term is coded once and includes a switch for the forward and backward cases. Similarly, for computing the right-hand side of Eqs. (7)-(9), there is an additional switch for forecast or nudging mode (i.e., exclude or include the gain term).

For an experiment, choose $G' = G = 1$, $\Delta x = 0.02$, $u = 0.5$, and $\Delta t = 0.025$. Per Eq. (7), the viscosity is $\upsilon = 4 \times 10^{-6}$. Pick a truth (or "nature") state of $q = \sin^2 \pi x$ but an experimental initial condition shown in Fig. 1, with values selected from a Gaussian distribution with a mean of 0 and a standard deviation of 0.05. Data are assimilated at all grid points and time steps.

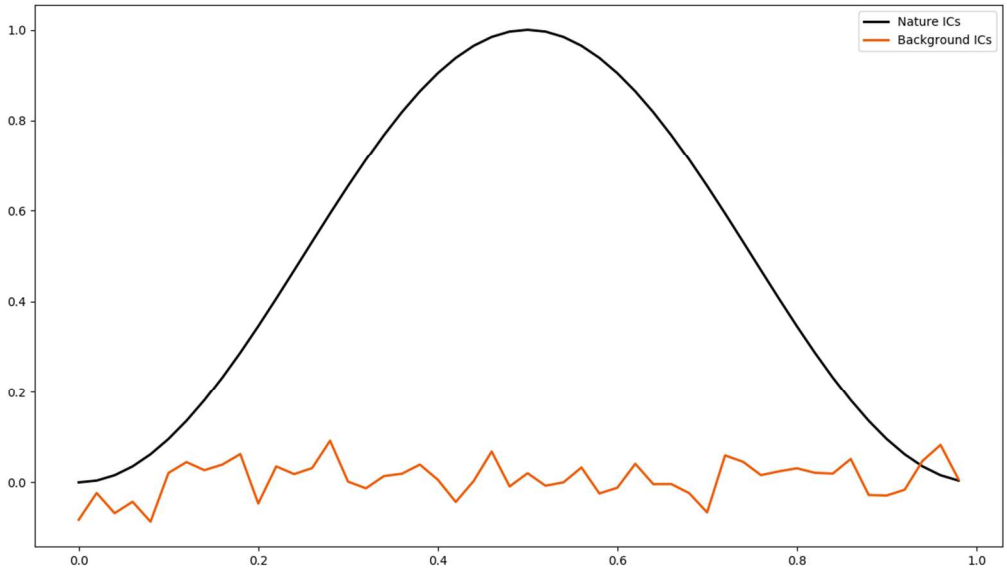

Fig. 1—The black line is the true initial condition, defined by $q = \sin^2 \pi x$. The orange line is the experimental initial condition, with values picked from a Gaussian distribution with a mean of 0 and a standard deviation of 0.05.

The analysis after one, two, and three pairs of DBFN forward and backward nudges is shown in Fig. 2. The analysis from the first pair of nudges resembles the truth. The analysis after the second pair of nudges offers only a small additional reduction in error. The analysis after the third pair of nudges is nearly identical to the second. The mean absolute error (MAE, $\sum_{i=1}^{N} |y_i - x_i|$) of the solution as a function of time is shown in Fig. 3, with blue used for forward nudges and red for backward nudges. Initial error is about 0.5 but quickly comes down in the first forward nudge. The first backward nudge also noticeably reduces error. After this, error is only slightly reduced, consistent with Fig. 2. The reason for the limited improvement appears to be the diffusive nature of the numerical scheme, discussed below.

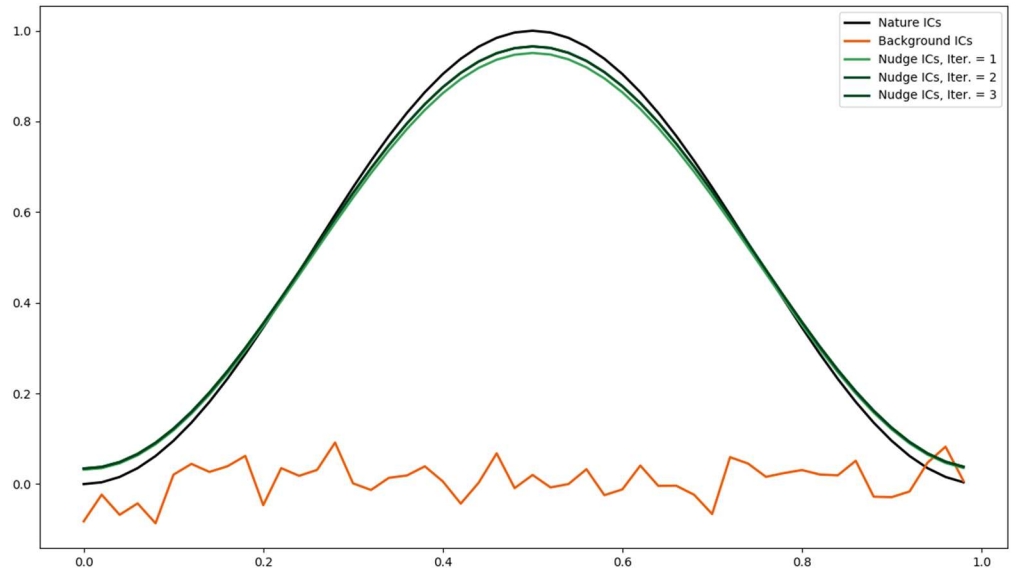

Fig. 2—DBFN solution analysis of one, two, and three pairs of back-and-forth nudges (green lines of light to dark intensity). The analysis after the third pair of nudges is nearly identical to the analysis after the second pair of nudges and is visually indistinguishable.

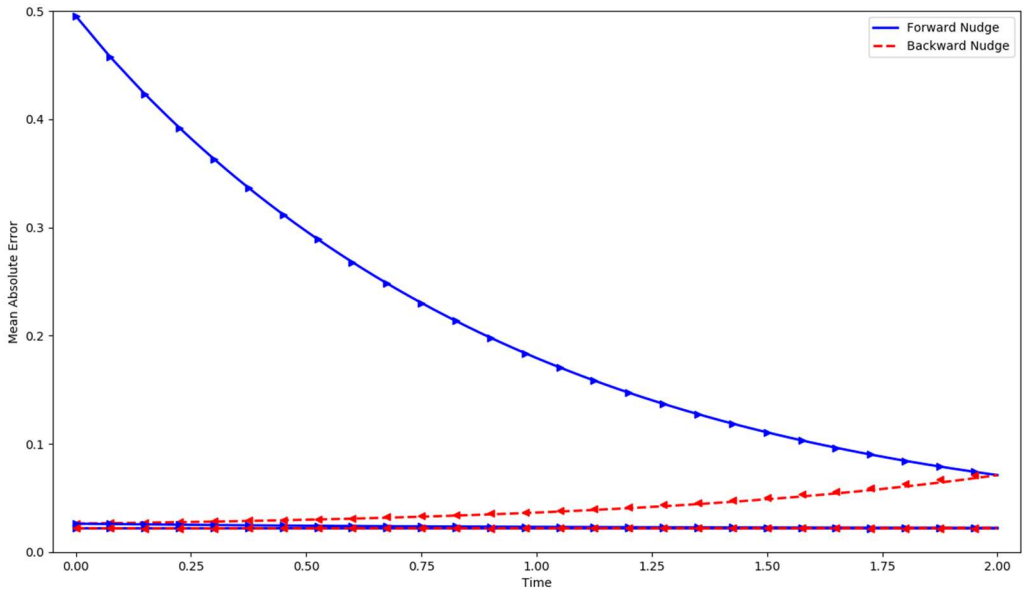

Fig. 3—Error as a function of time step. Blue shows error in forward nudge and red the error in backward nudge. The initial error is near the top of the figure, approximately 0.5.

A forecast is computed from the analysis following the third pair of nudges. The forecast is for the time interval from $t = 0$ to $t = 2$ (i.e., one period). Results are shown in Fig. 4. The truth is shown in black. Because Eq. (5) is nondiffusive and periodic, the truth at $t = 2$ is equal to the truth at $t = 0$. The forecasts initialized from the analysis and random initial conditions also are shown (green and orange, respectively). Because the numerical scheme is diffusive but the true system is not, the error in the forecast has increased from $t = 0$ to $t = 2$. This can been seen in the lower peak (cf. Figs. 2 and 4). How much of this error can be corrected by a second analysis cycle?

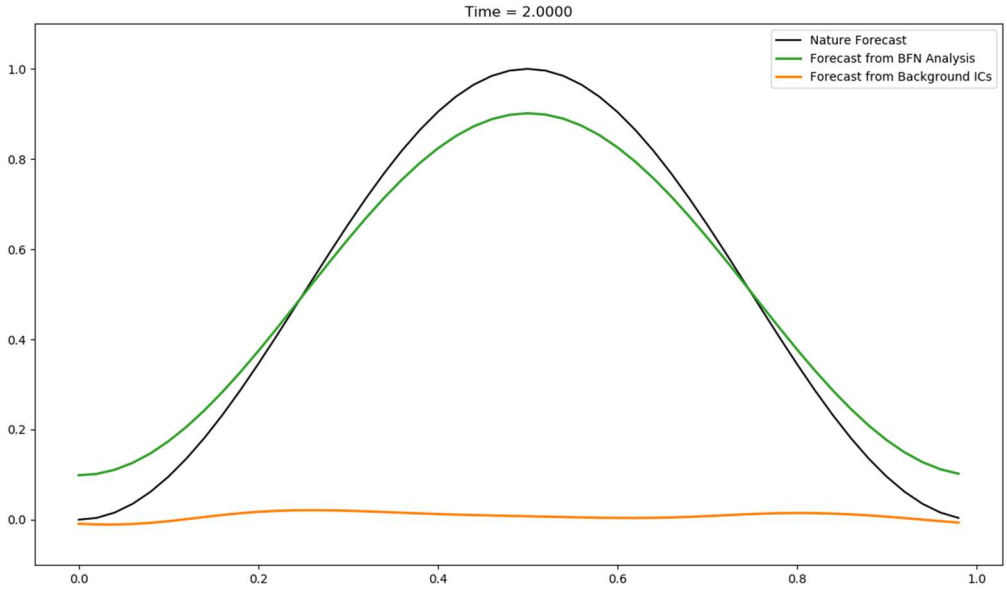

Fig. 4—Results at $t = 2$ for the Nature Run (green), forecast from analysis initial conditions (green), and forecast from original initial conditions (orange).

Running a second cycle reveals little improvement over the first analysis (Fig. 5). The analysis is computed from the forecast shown in Fig. 4 (green line). Three pairs of DBFN nudges are used. The second analysis is nearly identical to the first analysis (cf. Figs. 5 and 2). Through ten analysis-forecast cycles, the analysis error does not reduce (Fig. 6), due to the diffusive nature of Eq. (7). Additional tests with more pairs of nudges show similar results. It appears the diffusive nature of Eqs. (7)–(9) limits the accuracy of the system.

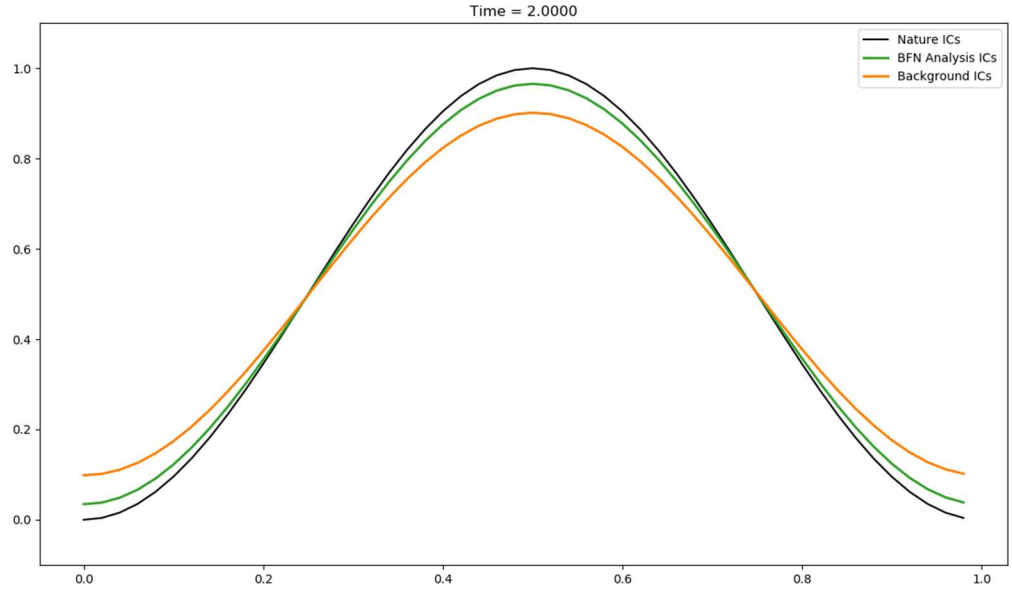

Fig. 5—Results of the second analysis. The Nature Run is shown in black, the background condition in orange (identically the green line in Fig. 4), and the resulting analysis in green. This second analysis is nearly identical to the first analysis (Fig. 2, dark green line).

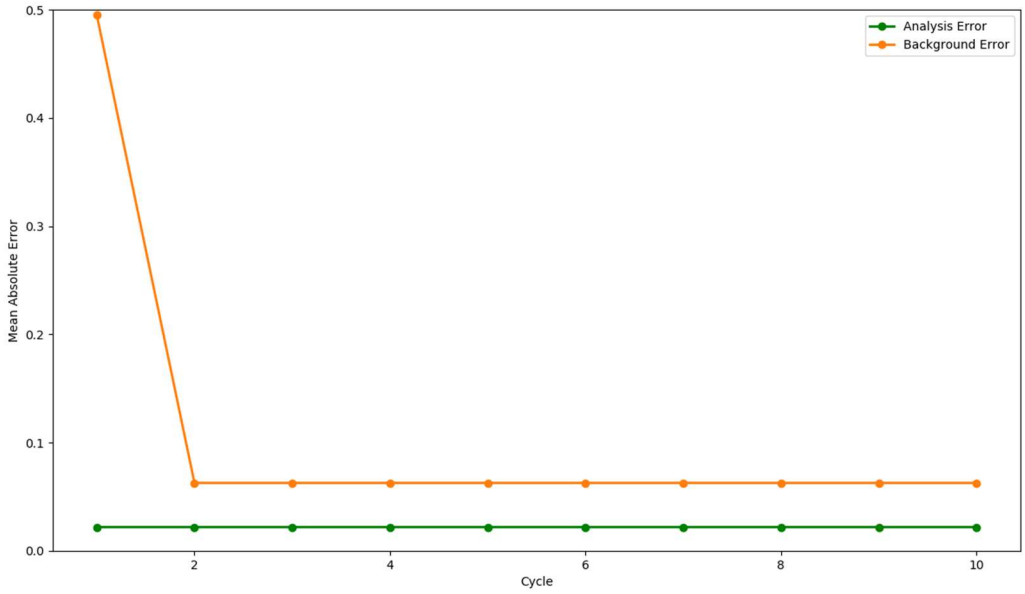

Fig. 6—MAE of background and analysis states over 10 analysis-forecast cycles (evaluated at analysis time). After the first cycle, errors do not reduce due to the diffusive nature of Eq. (7).

4. DBFN IN THE LORENZ 05 MODEL

For a second example, DBFN is implemented in the dynamical system described by Lorenz (2005). DBFN will be tested for one forecast cycle and will show the ability to reduce analysis errors to 0. Lorenz (2005) introduces a simple dynamical model that displays chaotic behavior, tunable small- and large-length scale variability, and slow and fast temporal modes of variability. Because of the chaotic behavior, it is sensitive to small perturbations (e.g., analysis error), and it has been widely used as a data assimilation testbed (e.g., Ngodock et al. 2020, Fairbairn et al. 2014, Ambadan and Yang 2009, Bishop et al. 2014). The dynamical equation is

$$\frac{d}{dt}X_n = [X,X]_{K,n} - X_n + F, \tag{10}$$

where $[X,X]_{K,n}$ (defined below) is the advection term, $-X_n$ is the diffusive term, and F is a selected forcing. The advection term is defined as

$$[X,Y]_{K,n} = \frac{1}{K^2}\sum_{j=-J}^{J}\sum_{i=-J}^{J}\left(-X_{n-2K-i}Y_{n-K-j} + X_{n-K+j}Y_{n+K+j}\right), \tag{11}$$

where $J = K/2$ and K is a selected smoothing parameter. Large K produces a spatial energy spectrum with a peak at long wavelengths. See Lorenz (2005) for more details.

For a numerical experiment, choose $F = 10$, $K = 8$, and the number of grid points $N = 240$. These are commonly used values (e.g., Ngodock et al. 2020). As with Eq. (5), periodic boundary conditions are used. For time stepping, use the Runge-Kutta fourth order accurate scheme (e.g., Press et al. 1992) with a time step of $\Delta t = \frac{1}{40}$. In Eq. (10), one unit of time is comparable to 5 days, per Lorenz (2005). For initial conditions, values are picked from a uniform random distribution between 0 and 1. The model is spun up for 10 years (720 time units). The model state during the tenth year of spin-up is shown in Fig. 7. Variability at multiple time and space scales is visible.

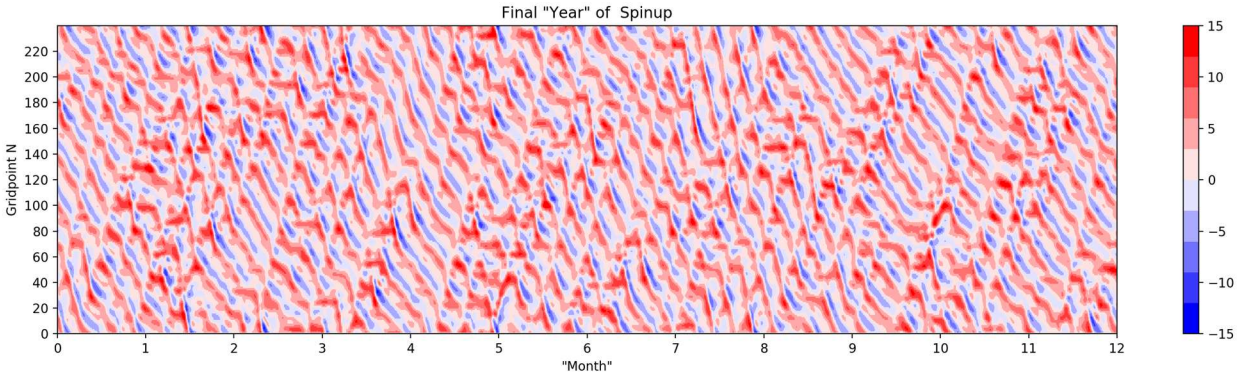

Fig. 7—Year 10 of spin-up of the Lorenz 2005 model. Multiple scales of variability are visible in space and time.

To test DBFN, set the background state identically equal to 0. The truth is taken as the model state at the end of spin up (Fig. 8). Data are assimilated at all grid points. Five pairs of back-and-forth nudges are used. Results, with different choices of gain G, are shown in Fig. 9. The choice of gain has a large impact. With small gain (G = 1), the analysis solution (purple) does not resemble the truth (green). In fact, the analysis is worse than the background, as will be discussed. An intermediate gain value (G = 5, blue line)

does resemble the truth. A large gain value ($G = 50$, orange line) nearly, but not identically, matches the truth.

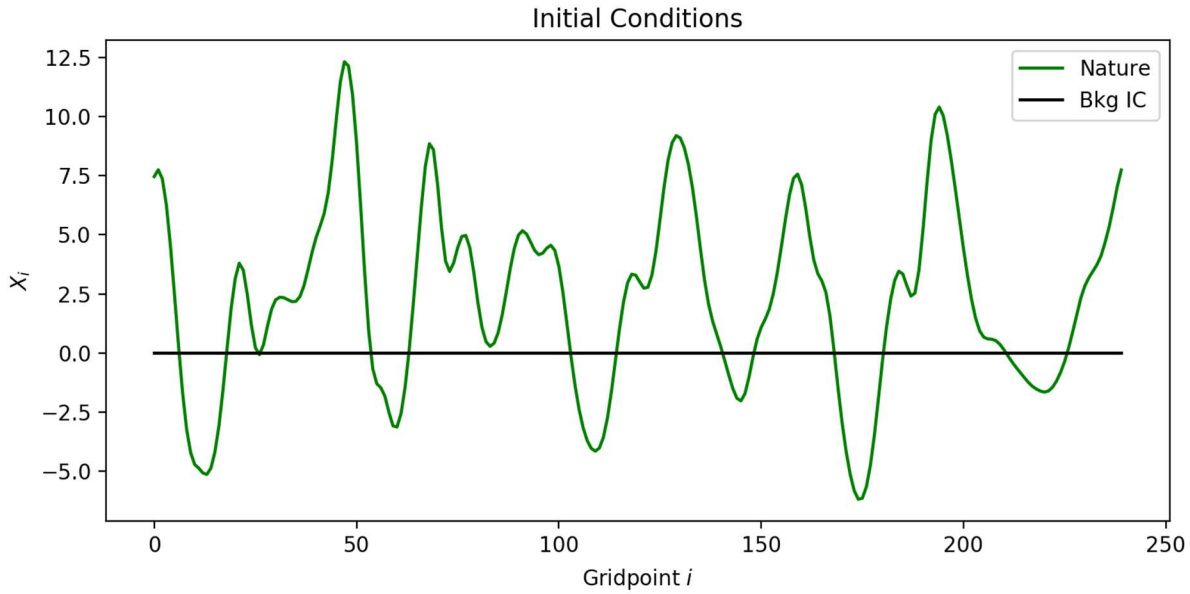

Fig. 8—Green line shows the true initial condition. Black line shows the background initial condition (identically 0).

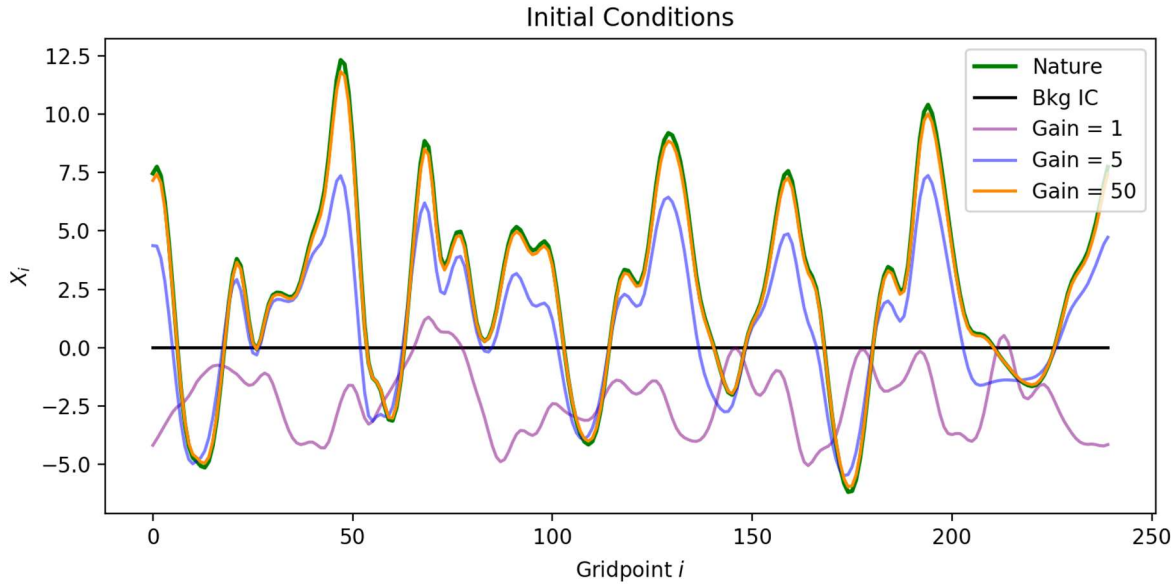

Fig. 9—Analysis state resulting from three different choices of gain, using background initial conditions of 0 (cf. Fig. 4.2).

Error evolution during the nudging process is examined now. Fig. 10 shows MAE of each gain case as a function of time. Results show only one pair of nudges is needed to minimize error. This may be due to the large amount of data available. Curiously, error tends to increase throughout the backwards nudge, particularly for the $G = 1$ case, for which the analysis error is much higher than the initial condition error

(i.e., the error level on the left-hand side of the graph). Perhaps this is because the diffusion term is working in opposition to the flow of time and the gain is relatively small. This issue also has been noted in the literature (Ruggerio et al. 2016). In the $G = 50$ case, error does not grow during the backwards nudge, perhaps because the gain is large.

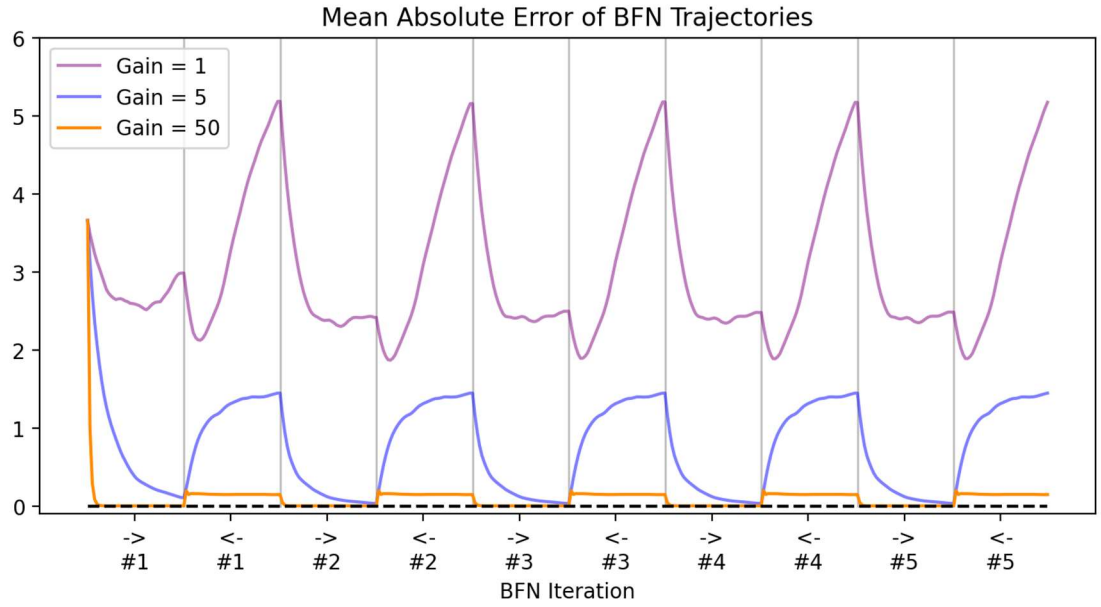

Fig. 10—For each choice of gain, MAE throughout the five pairs of nudging iterations. The gray vertical lines mark the switch between nudging directions. Nudging direction is indicated along the bottom axis by the arrows (forward: ->, backward: <-).

5. CONCLUSIONS

The DBFN method has provided accurate results in limited testing. Additional work is needed to establish its viability before testing in NCOM. Specifically, it needs to be compared with 3DVAR and 4DVAR methods in the Lorenz 2005 model. Prior work by Ngodock et al. (2020) can be leveraged there. Realistic data density needs to be used, which will necessitate identifying appropriate gain matrices (covariances), which is a challenging issue for data assimilation. If these results are promising, the next step would be to implement and test DBFN for NCOM.

6. ACKNOWLEDGMENTS

This work was funded through a Karles Fellowship, which is a Naval Innovative Science & Engineering (NISE) workforce development program. Discussions with and assistance from Dr. Hans Ngodock (Code 7321), Dr. Matt Carrier (Code 7321), Dr. Innocent Souopgui (University of New Orleans) were invaluable.

7. REFERENCES

1. Ambadan, J. T., and Y. Tang. 2009. "Sigma-Point Kalman Filter Data Assimilation Methods for Strongly Nonlinear Systems," *J. Atmos. Sci.,* 66, 261–285, https://doi.org/10.1175/2008JAS2681.1.

2. Auroux, D., J. Blum. 2005. "Back and forth nudging algorithm for data assimilation problems," *Comptes Rendus Mathematique,* **340**(12), pp. 873-878, doi: 10.1016/j.crma.2005.05.006.

3. Auroux, D., J. Blum, and M. Nodet. 2011. "Diffusive Back and Forth Nudging algorithm for data assimilation," *Comptes Rendus Mathematique,* **349**(15-16), pp.849-854.

4. Barron, C.N., A.B. Kara, P.J. Martin, R.C. Rhodes and L.F. Smedstad. 2006. "Formulation, implementation and examination of vertical coordinate choices in the Global Navy Coastal Ocean Model (NCOM)," *Ocean Modelling,* Vol. 11, pp. 347-375.

5. Bennett, A.F.. 2002. "Inverse modeling of the ocean and atmosphere" (Cambridge University Press).

6. Bleck, R. 2002. "An oceanic general circulation model framed in hybrid isopycnic-Cartesian coordinates." *Ocean Modelling,* **4**(1): 55-88, https://doi.org/10.1016/S1463-5003(01)00012-9.

7. Bishop, C.H., S. Frolov, D.R. Allen, D.D. Kuhl, and K. Hoppel. 2017. "The Local Ensemble Tangent Linear Model: an enabler for coupled model 4D-Var," *Q.J.R. Meteorol. Soc.,* 143: 1009-1020. doi:10.1002/qj.2986.

8. Coelho, E., G. Peggion, C. Rowley, G. A. Jacobs, R. Allard and E. Rodriguez. 2009. "A note on NCOM temperature forecast error calibration using the ensemble transform," *Journal of Marine Systems*, Vol. 78, S272-281.

9. Courant, R., K. Friedrichs, H. Lewy. 1928. "Über die partiellen Differenzengleichungen der mathematischen Physik," *Mathematische Annalen* (in German), **100**(1): 32–74, doi:10.1007/BF01448839.

10. Cummings, J.A., and O. M. Smedstad. 2013. "Variational Data Assimilation for the Global Ocean," *in Data Assimilation for Atmospheric, Oceanic and Hydrologic Applications,* Vol. II, Chapter 13.

11. Daley, R. and E. Barker. 2001. "NAVDAS: Formulation and diagnostics," *Monthly Weather Review,* **129**(4): 869-883.

12. Evensen, G. 1994. "Sequential data assimilation with a nonlinear quasigeostrophic model using Monte-Carlo methods to forecast error statistics," *J. Geophys. Res.,* 99, pp. 10143–10162.

13. Fairbairn, D., S.R. Pring, A.C. Lorenc, and I. Roulstone. 2014. "A comparison of 4DVar with ensemble data assimilation methods," *Q.J.R. Meteorol. Soc.,* 140: 281-294. doi:10.1002/qj.2135.

14. Leveque, R.J. 2002. "Finite volume methods for hyperbolic problems" (Cambridge University Press).

15. Lorenz, E.N. 2005. "Designing Chaotic Models," *J. Atmos. Sci.,* 62, 1574–1587, https://doi.org/10.1175/JAS3430.1.

16. Luenberger, D. 1966. "Observers for multivariable systems." *IEEE Transactions on Automatic Control,* **11**(2), pp.190-197.

17. Martin P.J. 2000. "Description of the Navy Coastal Ocean Model Version 1.0," NRL Report NRL/FR/7322-00-9962, 46 pp., https://apps.dtic.mil/dtic/tr/fulltext/u2/a387444.pdf.

18. Metzger, E.J., R.W. Helber, P.J. Hogan, P.G. Posey, P.G. Thoppil, T.L. Townsend, A.J. Wallcraft, O.M. Smedstad, D.S. Franklin, L. Zumudio-Lopez, and M.W. Phelps. 2017. "Global Ocean Forecast System 3.1 Validation Testing," NRL Report NRL/MR/7320--17-9722, https://apps.dtic.mil/dtic/tr/fulltext/u2/1034517.pdf (accessed 7 December 2018).

19. Ngodock, H., and M. Carrier. 2014. "A 4DVAR System for the Navy Coastal Ocean Model. Part I: System Description and Assimilation of Synthetic Observations in Monterey Bay." *Monthly Weather Review,* **142**(6): 2085-2107.

20. Ngodock, H., I. Souopgui, M. Carrier, S. Smith, J. Osborne, and J. D'Addezio. 2020. "An ensemble of perturbed analyses to approximate the analysis error covariance in 4dvar," *Tellus A: Dynamic Meteorology and Oceanography,* 72:1, 1-12, DOI: 10.1080/16000870.2020.1771069.

21. Oke, P.R., P. Sakov, M.L. Cahill, J.R. Dunn, R. Fiedler, D.A. Griffin, J.V. Mansbridge, K.R. Ridgway, and A. Schiller. 2013. "Towards a dynamically balanced eddy-resolving ocean reanalysis: BRAN3," *Ocean Modelling,* 67, pp.52-70.

22. Press, W.H., S.A. Tekolsky, W.T. Vetterling, and B.P. Falnnery. 1992. Numerical Recipes in Fortran, Second Edition, Volume 1 (Cambridge University Press).

23. Rowley, C., and A. Mask. 2014. "Regional and coastal prediction with the Relocatable Ocean Nowcast/Forecast System," *Oceanography,* **27**(3):44–55, https://doi.org/10.5670/oceanog.2014.67.

24. Ruggiero, G.A., Y. Ourmieres, E. Cosme, J. Blum, D. Auroux, and J. Verron. 2015. "Data assimilation experiments using diffusive back-and-forth nudging for the NEMO ocean model," *Nonlinear Processes in Geophysics,* **22**(2), pp.233-248.

25. Sakov, P., F. Counillon, L. Bertino, K.A. Lisæter, P.R. Oke, and A. Korablev. 2012. "TOPAZ4: an ocean-sea ice data assimilation system for the North Atlantic and Arctic," *Ocean Sci.,* 8, 633–656, https://doi.org/10.5194/os-8-633-2012.

26. Smith, S., H. Ngodock, M. Carrier, J. Shriver, P. Muscarella, I. Souopgui. 2017. "Validation and Operational Implementation of the Navy Coastal Ocean Model Four Dimensional Variational Assimilation System (NCOM 4DVAR) in the Okinawa Trough." *in Data Assimilation for Atmospheric, Oceanic and Hydrologic Applications,* Vol. III, Chapter 18.

27. Wei, M., G. Jacobs, C. Rowley, C.N. Barron, P. Hogan, P. Spence, O.M. Smedstad, P. Martin, P. Muscarella, E. Coelho. 2016. "The performance of the US Navy's RELO ensemble, NCOM, HYCOM during the period of GLAD at-sea experiment in the Gulf of Mexico." *Deep-Sea Research II*, 129, 374-393, http://dx.doi.org/10.1016/j.dsr2.2013.09.002